

EXPERIMENTAL STUDY OF A COMBINED STEEL LEAD DAMPER (PART. 2)

Yongshan ZHANG¹, Xueyuan YAN², Huanding WANG³ and Yajun XIN⁴

¹ Professor, Earthquake Engineering Research & Test Center, Guangzhou University, Guangzhou, China

² Ph. D. Student, School of Civil Engineering, Harbin Institute of Technology, Harbin, China

³ Professor, School of Civil Engineering, Harbin Institute of Technology, Harbin, China

⁴ Lecturer, School of Civil Engineering and Mechanics, Yanshan University, Qinhuangdao, China

Email: zhangys6411@163.com, yxy910@163.com

ABSTRACT :

An ingenious passive combined steel lead damper (CSLD) is presented. The damper is composed of steel sheet and lead. Processing technique of the damper is explored firstly. Then, mechanical property tests of CSLD of different sizes are carried out on press-shear machine, the results show that CSLD has full hysteresis loop and is of the same performance as low yield strength mild steel damper, geometry parameters of different values of CSLD all have influence on its hysteresis loop. Finite element entity modeling and simulation analysis for CSLD are performed using software ANSYS, and contrasted with the above tests results, which indicate they agree well with each other. Then, large numbers of simulation analyses of CSLD of different sizes are carried out, the simulation results and tests results are utilized for the polynomial regression of characteristic parameters of CSLD's restoring force model. The polynomials express relations between characteristic parameters of CSLD's restoring force model and geometry parameters of CSLD. Genetic algorithm is used to optimize the geometric parameters of CSLD according to the polynomials, a set of dampers of better energy dissipation capacity are gained. Finally, shaking table tests of a quarter-scale steel building model are carried out, the results of tests indicate that CSLD has full hysteresis loop and help to reduce the structural vibration effectively.

KEYWORDS:

combined steel lead damper, mechanical property test, polynomial regression of hysteretic characteristic parameters, parameter optimization using genetic algorithm, shaking table test

1. INTRODUCTION

Lead damper and mild steel damper are the two kinds of dampers which are studied maturely in the world. Massive works in this field are carried out and lots of research results are obtained^[1-9]. A combined steel lead damper (Figure 1) is presented in this paper based on the advantages of the above two kinds of dampers, and previous studies have been carried out^[10, 11]. Most of CSLDs are processed as I-shape, others are made in the shape of a line. In order to prevent corrosion from influencing the performance of CSLD and reduce maintenance quantity during service, the stainless steel plate is machined as I-shape and welded on the upper and bottom plates through argon-arc welding, and then the lead is melted and poured into the I-shaped formation. The lead is in complex stress state. There is no bond force between stainless steel plate and lead. The stainless steel plate is thin. Therefore a certain amount of restraint bolts are set on the web plate and flange of CSLD to ensure cooperative work of stainless steel plate and lead, and prevent stainless steel plate from buckling. Spacing of restraint bolts is designed according to the limit of width-thickness ratio when buckling failure of the stainless steel plate occurs.

The designed CSLDs always have large horizontal initial stiffness, low horizontal yield force and small vertical bearing capacity. In general case, the direction parallel to the web plate of the damper is defined as main direction, and the direction perpendicular to the main direction is called auxiliary direction. Working mechanisms of CSLD are: stainless steel plate offers initial stiffness while lead cord offers low yield force; the

combined web plate receives shear force and the combined flange flexes when outer force acts on in the main direction; the combined flange receives shear force and the combined web plate flexes when outer force acts on in the auxiliary direction. Shearing members of the damper offer large hysteretic force under small displacement; flexural members also provide hysteretic force when greater displacement occurs.

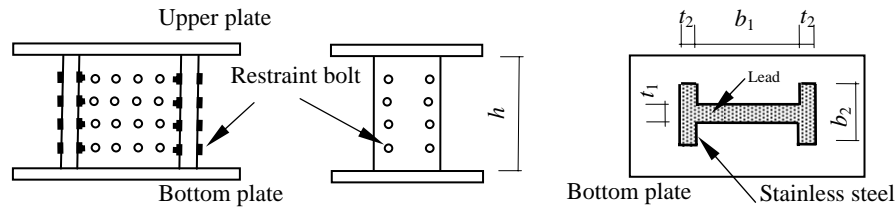


Figure 1 Constitution figure of CSLD

2. Processing technology of CSLD

In order to make use of the advantages of the two materials and ensure stable hysteretic force, thinner stainless steel plate was used in the study. Thus, there was problem with the connection between the stainless steel plate and the upper and bottom plates. It is necessary to study the processing technology of CSLD.

2.1 Connection mode of clamping

On the damper, thick steel plate (3 mm thickness) was welded on the upper and bottom plates. The web plate and flange of the I-shaped stainless steel formation and the thick steel plate were connected through little bolts. The construction and the test phenomenon are shown in Figure 2. Results of tests indicated that the little bolts at the upper and bottom ends of the damper received bigger shear force and damaged before the damper itself worked. The failure mode of the damper is shown in Figure 2(c). Therefore the connection mode of clamping is unusable.

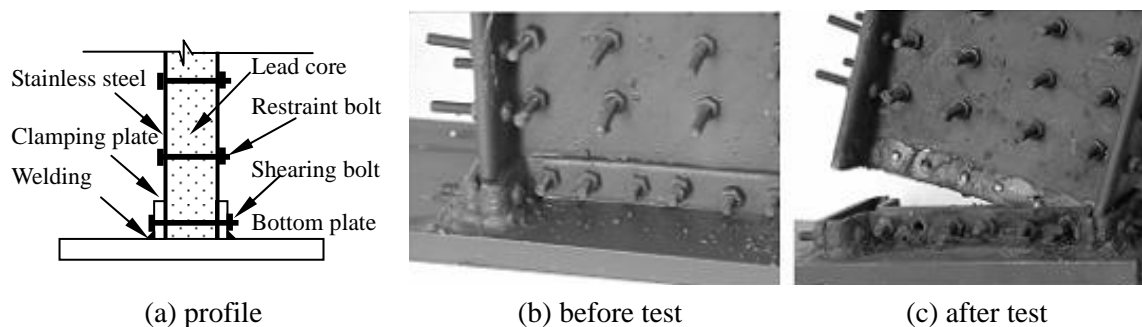


Figure 2 Connection mode of clamping

2.2 Connection mode of pressure

An improved processing technology was presented based on the analysis for failure cause of connection mode of clamping, that is, connection mode of pressure. On the premise that ensured the size of the main body of the damper, the upper and bottom ends of the stainless steel plate were folded outward, and then the folded parts were pressed on the upper and bottom plates using thick steel plate, the thick steel plate and the upper and bottom plates were connected together via high-strength bolts and welding. The construction and the test phenomenon are shown in Figure 3. Results of tests showed that the web plate could work well and dissipate energy, but the joint of the flange and the upper and bottom plates turned out to be hinge joint (Figure 3(c)), which indicated that the function of the flange didn't realize well. Therefore the connection mode of pressure is

unusable.

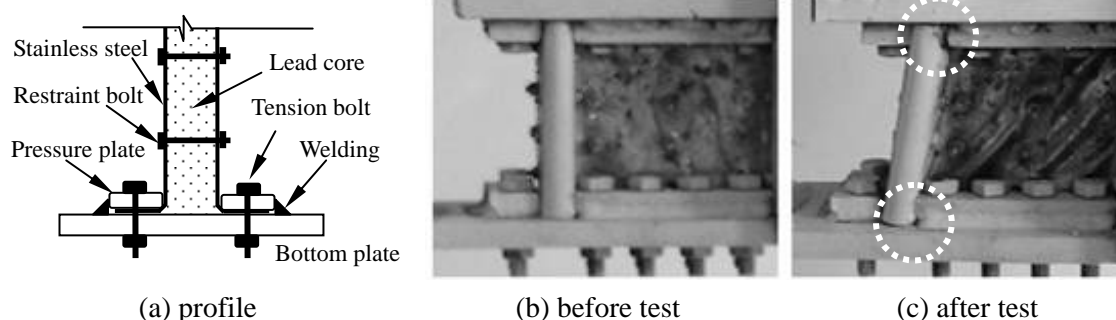


Figure 3 Connection mode of pressure

2.3 Connection mode of argon-arc welding

The stainless steel plate was welded directly on the upper and bottom plates using argon-arc welding. The construction and the test phenomenon are shown in Figure 4. Results of tests indicated that the connection using argon-arc welding was reliable. The web plate and the flange of the damper could work well. The advantages of the two materials were made use of fully. The disadvantage was that the stainless steel plate couldn't be too thin, which wasn't beneficial to the welding. It was acceptable that thickness of the stainless steel plate was larger than 8 mm. The melting point of lead is low (327.4°C), and lead will melt at high temperature. Therefore, the stainless steel plate was processed as I-shape and welded on the upper and bottom plates, and then the melted lead was poured into through the small hole on the upper and bottom plates, the hole was drilled beforehand. Slitting test showed that the damper was replete with lead. Therefore the connection mode of argon-arc welding is feasible.

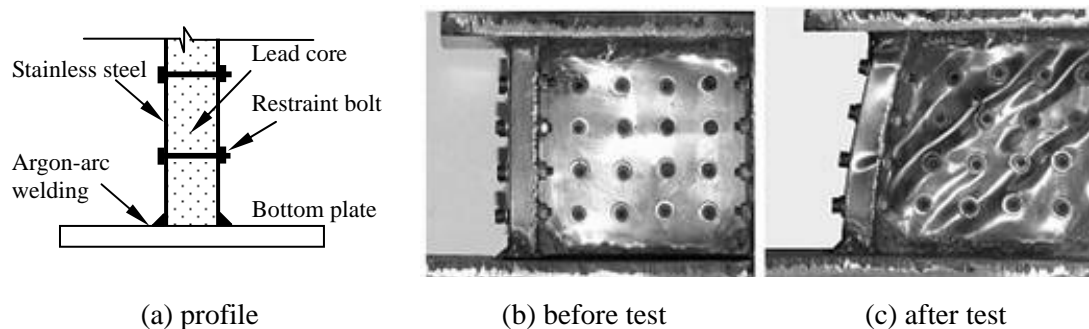


Figure 4 Connection mode of argon-arc welding

3. Performance tests of CSLDs

3.1 Damper designing and operating modes

12 dampers shown in Table 1 were designed for the study of the influences of parameters on the properties of the damper. Pseudo-static tests of these dampers were carried out using electro-hydraulic servo press-shear machine. The machine is mainly composed of vertical jack and horizontal electro-hydraulic servo actuator. CSLD is displacement related damper, the influence of loading frequency on the properties of the damper is small. In order to study the main performances of the damper, cyclic tests were performed and the loading frequency was 0.5 Hz, considering the frequency responses of the test equipment. In the tests, vertical load was zero; displacement-controlled mode was adopted; the horizontal displacement were ± 5 mm and ± 10 mm

respectively, and there were three loading cycles in each operating mode. Testing direction was the main direction of the damper.

Table 1 Design parameters of CSLD

Damper No.	Steel thickness t (mm)	Web thickness t_1 (mm)	Flange thickness t_2 (mm)	Web width b_1 (mm)	Flange width b_2 (mm)	Damper high h (mm)
1	1.0	20	15	150	0	150
2					80	
3					120	
4		15	15	150	80	150
5		25				
6		30				
7	1.5	25	20	150	0	150
8					80	
9					120	
10		20	20	150	80	150
11		30				
12		35				

3.2 Results and analyses of tests

It could be observed from the test phenomena that the failure process of the damper could be divided into three stages. At the initial loading stage, there weren't obvious differences of the damper before and after the test. The stress-strain relationship of the damper was at the elastic stage. With the load increased, when it was larger than the yield force, the damper was at the nonlinear stage, and there was a phenomenon that the stainless steel plate buckled. The buckling was at an angel of forty-five degrees. But the bearing capacity of the damper still could be increased. Although the inner lead yielded, when there was tiny displacement out of plane because of the buckling of the stainless steel plate, there was also membrane tensile stress on the web plate. Therefore the damper could accept larger load. This phenomenon could be explained by the tension field theory. When carried out destructive test of larger displacement, the horizontal welding seams at the ends of the flange and the vertical welding seams of the flange cracked or the buckled stainless steel plate failed firstly because of excessive membrane tensile stress. The typical failure modes of the damper are shown in Figure 5.

During the test, high-strength bolts were used for the connection between the damper and the test equipment. The test displacements were small. The fixation of the base of press-shear machine was not firm. There are errors with the actuator. There are gaps between high-strength bolts and bolt holes. These uncertain factors existed. Therefore the maximum test displacements were not totally ± 5 mm and ± 10 mm.

Figure 6 shows the comparison for the load-displacement relationships of the No. 1, 2, 3 and No. 7, 8, 9 dampers. It also indicates the influence of flange width on the property of the damper. In the comparison figure of No. 1, 2 and 3, the flange of No. 2 damper is 80 mm wider than that of No. 1 and therefore the yield force of No. 2 damper is bigger than that of No. 1. The flange of No. 3 damper is only 40 mm wider than that of No. 2 and therefore the yield force of No. 3 damper is a little bigger than that of No. 2. The wider the flange is, the fuller the hysteresis loop is and the bigger the area of the hysteresis loop is. It can be observed from the comparison figure of No. 7, 8 and 9 that the variation of the flange width has little influence on the hysteresis loop. The flange of No. 8 damper is 80 mm wider than that of No. 7 and therefore the yield force of No. 8 damper is a little bigger than that of No. 7. The flange of No. 9 damper is only 40 mm wider than that of No. 8 and therefore the yield force of No. 9 damper is almost not bigger than that of No. 8. The reasons why the variation of the flange width has little influence on the properties of No. 7, 8 and 9 dampers while it has bigger influence on the properties of No. 1, 2 and 3 dampers are, the section areas of No. 7, 8 and 9 dampers are larger than that of No. 1, 2 and 3 dampers, the stainless steel plate thicknesses of No. 7, 8 and 9 dampers are thicker than that of No. 1, 2 and 3 dampers, which indicate that the main energy dissipation component of the damper is

the shear member and the influence of the flange width on the property of the damper is reduced with the section area is increased.

Figure 7 shows the comparison for the load-displacement relationships of the No. 4, 5, 6 and No. 10, 11, 12 dampers. It also indicates the influence of web thickness on the property of the damper. It can be seen from the comparison figure of No. 4, 5 and 6 that the yield force increases with the web thickness increases, which indicates that the thicker the web plate is, the stronger the energy dissipation capacity is. In the comparison figure of No. 10, 11 and 12, there aren't obvious increases with the yield force and the energy dissipation capacity as the web thickness increases. The reasons for the above phenomena are, the thickness of stainless steel plate of No. 10, 11 and 12 is 1.5 mm, the effect of the stainless steel increases, the effect of the additional lead decreases, and the influence of the web thickness of No. 10, 11 and 12 is not so obvious as which of No. 4, 5 and 6. It also can be observed from the above test curves that the dampers have steady and full hysteresis loops, which indicates strong energy dissipation capacity of the damper.

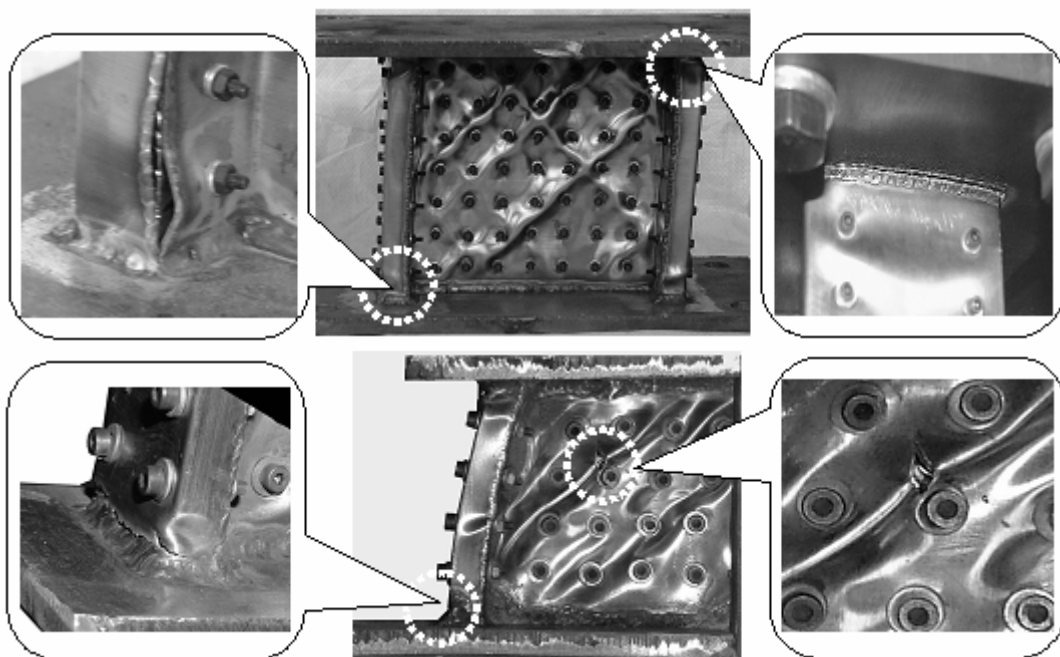


Figure 5 Failure mode of CSLD

4. Numerical analyses of CSLD

Numerical analyses for CSLD were carried out using finite element analysis software ANSYS. According to the construction requirements of the damper, solid element SOLID45 and shell element SHELL181 were chose for simulating lead and stainless steel respectively, contact element CONTA173 and target element TARGE170 were chose for simulating the interaction of the two materials. The model of bilinear kinematic hardening was chose as the mechanical model of the two materials according to their material characteristics.

The analysis process for CSLD is generally divided into four steps. Firstly, appropriate types of elements are chose in the software through the analyses for the boundary condition and the stress characteristics of the damper. Secondly, define real constants for every element according to the real sizes of the damper. Thirdly, define material properties for the used three kinds of materials. Finally, appropriate connection modes are chose for the connections between components of the damper, and the solid model is meshed. The restraint bolts are small and more. The memory space and the computing speed of the computer are affected by the total number of the meshed elements. Therefore in order to increase computing speed and reduce memory space, the restraint effect of the little bolts is simulated through the coupling of the node freedoms, and then the total number of the

meshed elements is reduced greatly, the error of the simulation is acceptable.

Tests of ± 5 mm and ± 10 mm displacement in the main direction of the damper were performed. Results of time domain load-displacement were read via the time-history postprocessor. Parts of the comparison curves between numerical analyses and tests are shown in Figure 8. The figure shows that they coincide with each other and the hysteresis loops can be simplified as bilinearity.

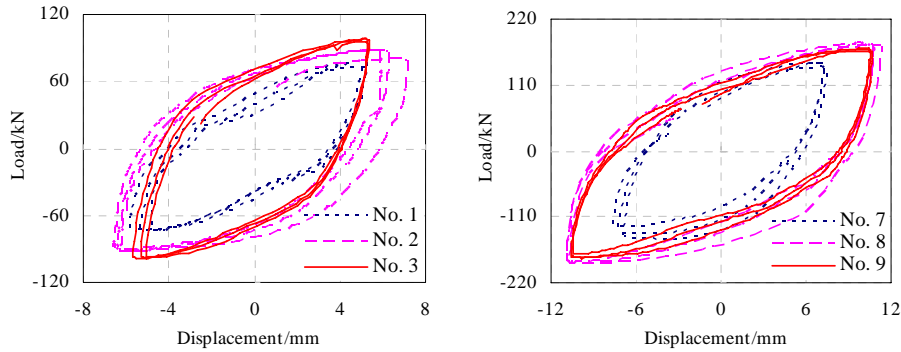


Figure 6 Influence of flange width on performance of CSLD

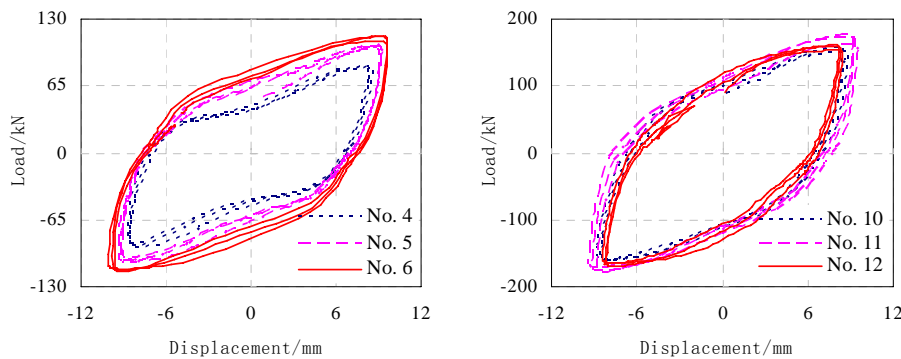


Figure 7 Influence of web thickness on performance of CSLD

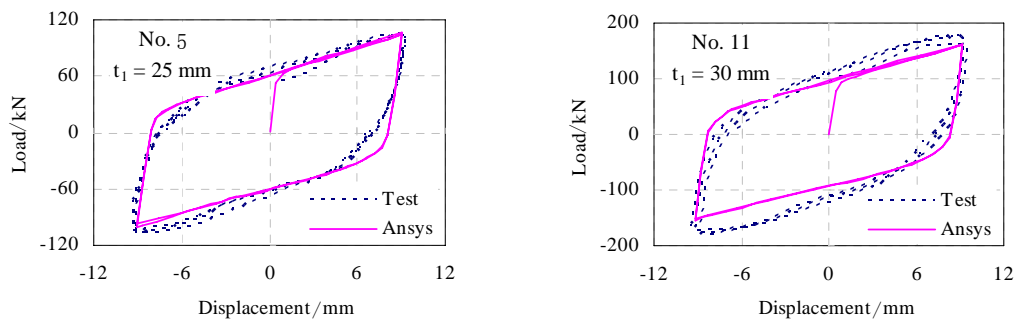


Figure 8 Comparisons between test and ANSYS analysis results

5. Polynomial regressions for the characteristic parameters of CSLD^[10]

From the above comparisons for the results of the tests and the ANSYS analyses, we know that the modeling for CSLD in the software is correct. Therefore large numbers of analyses for CSLD of different sizes are carried out. Polynomial regressions for the bilinear characteristic parameters of CSLD are performed using the numerical analysis data and the test data. The bilinear characteristic parameters are the yield force F_y , the elastic stiffness K_1 and the yield stiffness ratio K_2/K_1 . The polynomial expressions for the parameters are shown in Eqns.

5.1-5.3.

$$F_y = 328.22 + 335.63t - 147.65t^2 + 17.02t^3 + 0.303b_1 + 0.684t_1 + 2.75 \times 10^{-3}b_2^2 - 6.76 \times 10^{-6}b_2^3 + 1.81t_2 - 11.3h + 7.3 \times 10^{-2}h^2 - 1.57 \times 10^{-4}h^3 \quad (\text{kN}) \quad (5.1)$$

$$K_1 = 781 + 124t + 0.646b_1 + 1.37 \times 10^{-4}t_1^3 + 0.756b_2 - 4.77 \times 10^{-3}b_2^2 + 7.8910^{-6}b_2^3 + 2.24 \times 10^{-2}t_2^2 - 17.8h + 0.112h^2 - 2.34 \times 10^{-4}h^3 \quad (\text{kN/mm}) \quad (5.2)$$

$$K_2 / K_1 = 28.1 - 0.127t^3 - 0.0342b_1 + 6.08 \times 10^{-5}b_1^2 - 0.0301b_2 + 3.23 \times 10^{-4}b_2^2 - 6.47 \times 10^{-7}b_2^3 - 0.229h + 6.49 \times 10^{-4}h^2 \quad (\%) \quad (5.3)$$

where t is the thickness of the stainless steel plate; b_1 is the width of the web plate; t_1 is the thickness of the web plate; b_2 is the width of the flange; t_2 is the thickness of the flange; h is the height of the damper. It is necessary to point out that the above expressions have applicable ranges which are shown in Table 2.

Table 2 The range of every variable (unit: mm)

Variable	Range	Variable	Range
Steel thickness t	0.5-2.0	Web width b_1	70-367
Web thickness t_1	4-85	Flange width b_2	14-392
Flange thickness t_2	2-56	Damper high h	75-210

6. Optimization for the characteristic parameters of CSLD

The performance parameters of damper are generally obtained via cyclic testing. The energy dissipation capability of damper is judged according to the area of the hysteresis loop. In this study, the criterion that the area sizes of the hysteresis loops under the same load of 200 kN was proposed, the criterion was used for judging the energy dissipation capabilities of the dampers. Meanwhile, dampers of good energy dissipation capability need to satisfy the following conditions.

- (1) The yield force of the damper should be as small as possible, and the elastic stiffness should be as large as possible, so that the damper can dissipate the input energy as much as possible under small displacement.
- (2) The stiffness ratio should be as small as possible in order to increase the area of hysteresis loop. It can be observed from the results of the tests and the ANSYS analyses that the ratio ranges from 2% to 10%.

Based on the above considerations and the bilinear simplification for the restoring force model of the damper, the relationship between the yield force F_y , the elastic stiffness K_1 , the stiffness ratio K_2/K_1 and the area of the hysteresis loop S is shown in Eqn. 6.1.

$$S = 4F_y \times (F - F_y) \times (100 - K_2/K_1) / K_2 \quad (6.1)$$

where F is the output force of the damper; K_2 is the yield stiffness.

It is a problem that what values the six geometry parameters are and make the damper of better energy dissipation capacity. The total number of dampers of different sizes is huge. Therefore it is impossible to study every damper and screen out the desired dampers. Nature of all the optimization problems can be come down to searching a set of values of design variables to make design targets of design object optimized under certain constraints. The parameter optimization here is different from the general optimization. It is not to search a

unique set of values of variables, but to find out several set of values and make the values of the design targets close to the optimal value. The several set of values are standardized according to the elastic stiffness and the yield force of the damper, which provides a reference for the engineering application of CSLD.

The solution space which is composed of the ranges of the variables shown in Table 2 is divided into 3^6 subspaces uniformly, that is, the range of every variable is trisected. Then, local optimization in each subspace is obtained. Therefore there are 3^6 dampers for choice, which is beneficial to the serialization of the damper. Parameter optimization is carried out using MATLAB genetic algorithm tool and self-compiling program. The tool always tries to search the minimum of the fitness function, and therefore the opposite number of the area of the hysteresis loop is used as fitness function. The number of independent variables is 6. Energy dissipation through shear deformation is the main function of the damper. Therefore the geometry parameters should be constrained appropriately to avoid undesired deformation, and the following constraints are introduced.

$$\begin{cases} t_1 - b_2 \leq 0 \\ -t_1 + t_2 \leq 0 \\ -b_1 + b_2 - 2t_2 \leq 0 \end{cases} \quad (6.2)$$

Population size is 20. Random initial population is created in every subspace with a uniform distribution function. Maximum number of iterations the genetic algorithm performs is specified as 200. Crossover fraction is set to 0.6. Mutation function is specified as “Adaptive feasible”. Then run the solver until the iteration is around 100, the iteration converges. Run the solver 10 times and average the results. Considering the above conditions (1) and (2), 15 representative dampers are chose from the final optimized results and shown in Table 3.

Table 3 Representative CSLDs in the optimizing results using genetic algorithm (unit: mm)

Factor No.	Steel thickness	Web width	Web thickness	Flange width	Flange thickness	Damper high	Hysteretic area/kN·m	Maximum displacement
D-1	0.8	128	30	105	20	165	7.80	44.63
D-2	0.9	141	31	89	20	172	7.93	36.78
D-3	1.0	169	31	52	20	165	8.05	32.38
D-4	1.0	169	36	140	12	176	7.03	22.8
D-5	0.9	155	58	74	18	165	7.55	27.78
D-6	1.0	169	58	58	15	175	7.83	27.17
D-7	0.5	268	38	140	38	177	5.42	16.51
D-8	1.0	228	31	52	20	175	8.23	26.31
D-9	0.9	268	31	52	20	176	7.97	24.86
D-10	1.5	169	31	58	12	175	6.96	24.33
D-11	1.5	183	22	140	20	165	4.54	10.78
D-12	1.2	268	31	58	2	175	8.76	29.13
D-13	1.5	234	31	54	7	120	3.96	11.66
D-14	1.5	268	26	50	20	165	6.10	14.02
D-15	2.0	268	58	58	20	177	5.79	12.02

7. Shaking table tests of the structure with CSLD

7.1 Performance tests of the small size CSLD

Pseudo-static tests for the small size CSLD were carried out using electro-hydraulic servo press-shear machine. The sizes of the damper are shown in Table 4. Testing directions were the main direction and the auxiliary

direction of CSLD. Loading amplitudes were 5 mm and 10 mm, loading frequency was 0.1 Hz, and there were three loading cycles in each operating mode. During the tests, connections between test equipments must be firm, and errors caused by kinds of factors must be reduced, otherwise the experimental data measured would be unusable because hysteretic force of the damper is far lower than the maximum output of the equipments. Load-displacement curves of CSLD in the main and auxiliary directions are shown in Figures 9 and 10 respectively. The figures show that CSLD has full hysteresis loops which indicate good energy dissipation capability of the damper.

Table 4 Values of variables of CSLD for testing (unit: mm)

Variable	Value	Variable	Value
Steel thickness t	0.8	Web width b_1	60
Web thickness t_1	8	Flange width b_2	40
Flange thickness t_2	8	Damper high h	160

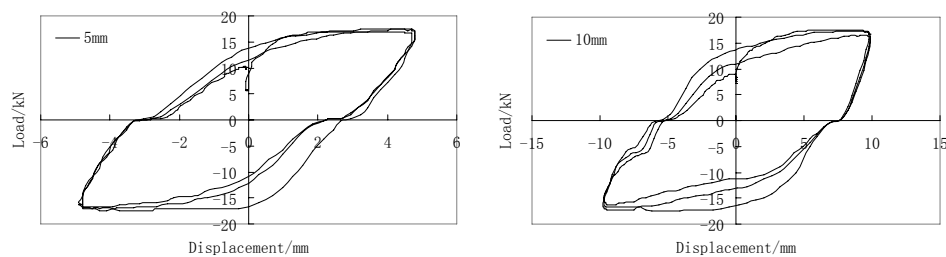


Figure 9 Load-displacement curves of CSLD in the main direction

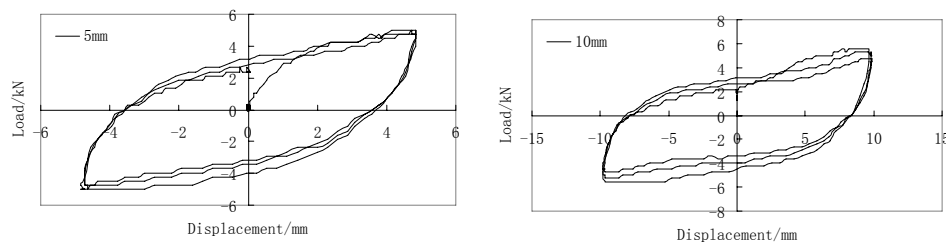


Figure 10 Load-displacement curves of CSLD in the auxiliary direction

7.2 Shaking table tests

The structural dimensions are 1.2 m×2.0 m in plane and 1.0 m in height, the structural weight is 0.3 t, counterweight is 3.93 t, and total weight is 4.23 t. The damper was fixed between layers via brace, and the main direction of the damper coincided with the long span direction of the model, that is, Y direction of the shaking table. Shearing rigidities of the brace in the long and short span directions are larger than rigidities of the damper in the corresponding directions. There were type 4381V acceleration transducers from Danmark on the structure and shaking table, they were used for collecting acceleration and displacement signals. There were laser displacement sensors between layers for collecting displacement signals.

90° and 180° components of Mexico ground motion measured at La Union seismic station in 1985 were chose as input ground motions in X direction and Y direction of the shaking table, the sample interval of the ground motion was 0.01 s. Amplitudes of the ground motion were modulated to 70 gal, 200 gal and 400 gal respectively according to *Code for seismic design of buildings*^[12], and the ratio for amplitudes of the two input directions was 1:0.85. Shaking table tests of the model structure with CSLD (controlled structure) and without CSLD (uncontrolled structure) were performed.

Figures 11 and 13 show the comparisons for time history curves of structural inter-story displacement between controlled and uncontrolled structure in the two directions respectively. Figures 12 and 14 are the comparisons

for time history curves of structural acceleration between controlled and uncontrolled structure. Table 5 lists values of control effects for structural inter-story displacement and acceleration reactions under kinds of working conditions, which are aseismic ratios. From the figures and table, it is observed good control effects of CSLD towards structural seismic responses in the two directions. After installing CSLD, structural inter-story displacement reactions are reduced obviously: maximum aseismic ratio is 66.1% in X direction, 53.8% in Y direction. Structural acceleration reactions in the two directions are also controlled well: maximum aseismic ratio is 30.9% in X direction, 26.1% in Y direction. Under frequent earthquake action, the damper does not dissipate energy obviously, and therefore control effects for structural acceleration reactions are poor; under fortification intensity and rare earthquake action, there are obvious control effects. The control effects for structural inter-story displacement and acceleration reactions in Y direction are worse than that in X direction, which relates to structural Y direction corresponding to the main direction of the damper, and the bigger rigidity of the damper in that direction.

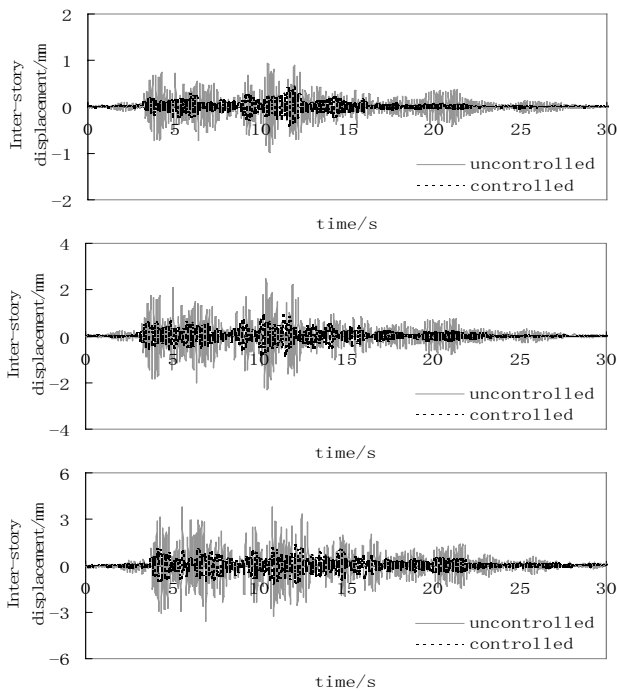


Figure 11 Time-history curves of structural inter-story displacement in X-direction

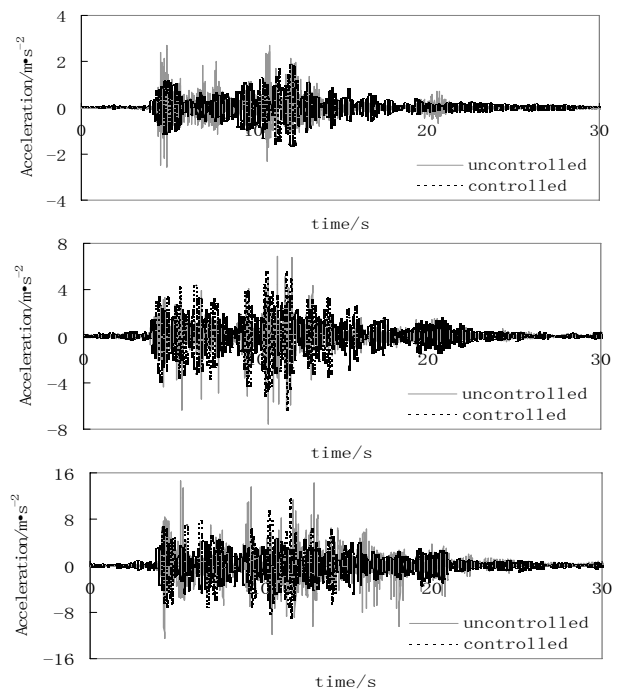
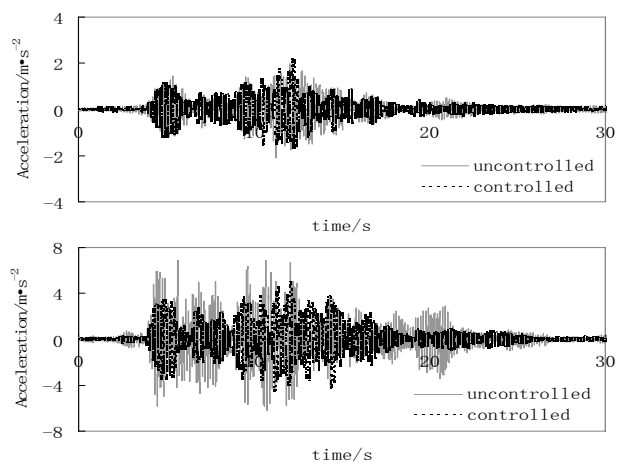
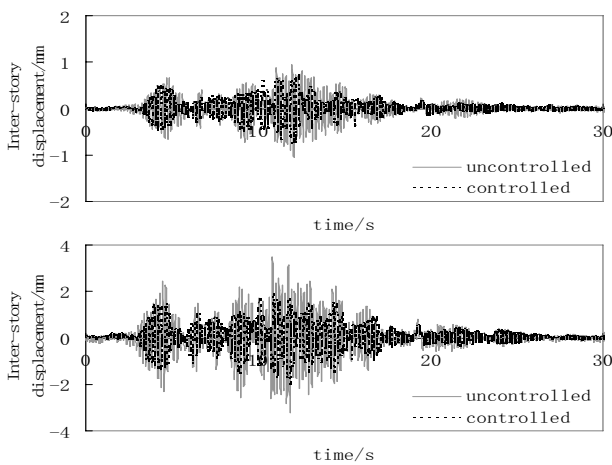


Figure 12 Time-history curves of structural acceleration reaction in X-direction



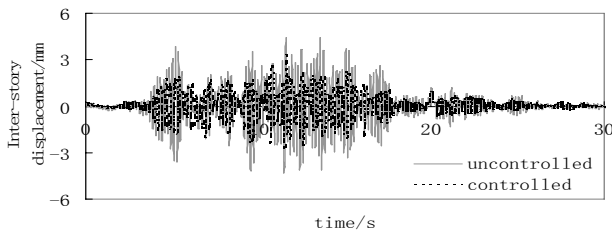


Figure 13 Time-history curves of structural inter-story displacement in Y-direction

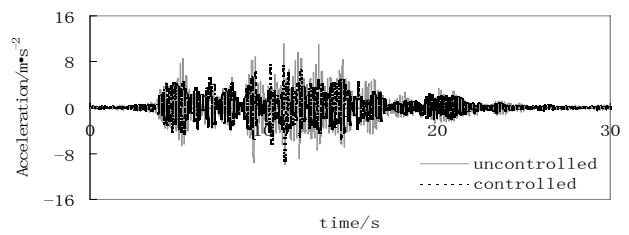


Figure 14 Time-history curves of structural acceleration reaction in Y-direction

Table 5 Control effects of damper for structural seismic responses under kinds of working conditions

Ground motion	Input direction	Peak value /gal	Control effect of displacement	Control effect of acceleration
Mexico	X	70	55.7%	30.9%
	Y	59.5	16.7%	-3.2%
Mexico	X	200	66.1%	11.9%
	Y	170	53.8%	26.1%
Mexico	X	400	62.5%	21.7%
	Y	340	24.1%	15.0%

8. Conclusions

In this study, we studied the seismic performance of the presented CSLD. Large numbers of experimental and theoretical studies were carried out, and then the following conclusions were obtained:

- (1) Processing technique of the damper was studied. Results of tests indicated that the connection using argon-arc welding was reliable. The web plate and the flange of the damper could work well. The advantages of the two materials were made use of fully. The disadvantage was that the stainless steel plate couldn't be too thin.
- (2) Pseudo-static tests for CSLDs of different sizes were carried out using press-shear machine. The results indicated that CSLD had full hysteresis loops and had the same performances as mild steel damper. Geometry parameters of different values had influence on the hysteresis loops of the damper.
- (3) Finite element entity modeling and numerical analysis of CSLD using finite element software ANSYS were performed. The results were compared with the results of tests, which showed that they coincided with each other and the modeling was correct.
- (4) Large numbers of numerical analyses for CSLD of different sizes were carried out, and the results together with the test results were used for the polynomial regressions of characteristic parameters of CSLD, and then the polynomial expressions were obtained.
- (5) Optimization for the geometry parameters of CSLD were performed using genetic algorithm and the polynomial expressions. A set of dampers of better energy dissipation capacity were gained.
- (6) Shaking table tests for a 1:4 scale steel structure model with CSLD and without CSLD were carried out. Results showed that CSLD had full hysteresis loops and had obvious vibration control effect. Seismic responses of the structure in the two directions were reduced effectively.

REFERENCES

1. Kelly J M, Skinner R I, Heine A J. (1972). Mechanisms of energy absorption in special devices for use in

- earthquake resistant structures. *Bulletin of New Zealand National Society for Earthquake Engineering* **5: 3**, 63-88.
2. Whittaker A S, Bertero V V, Thompson C L. (1991). Seismic testing of steel plate energy dissipation devices. *Earthquake Spectra* **7: 4**, 563-604.
 3. Ou Jinping, Wu Bo, Soong T T. (1996). Recent advances in research on application of passive energy dissipation systems. *Earthquake Engineering and Engineering Vibration* **16:3**, 72-96
 4. Yasushi Kurokawa, Mitsuo Sakamoto, Toshikazu Yamada, Haruhiko Kurino, Akihiro Kunisue. (1998). Seismic design of a tall building with energy dissipation damper for the attenuation of torsional vibration. *The Structural Design of Tall Buildings* **7:1**, 21-32.
 5. Masayoshi Nakashima, Satoshi Iwai, Mamoru Iwata, Toru Takeuchi, Shinzo Konomi, Takashi Akazawa, Kazuhiro Saburi. (1994). Energy dissipation behaviour of shear panels made of low yield steel. *Earthquake Engineering & Structural Dynamics* **23-12**, 1299-1313.
 6. Soong T T, Dargush G F. (1997). *Passive energy dissipation systems in structural engineering*, John. Wiley & Sons, New York.
 7. Wang Yanwu, Wang Tieying, Wang Huanding. (2004). Experimental research on two kinds of lead dampers. *Earthquake Engineering and Engineering Vibration* **24:1**, 166-171.
 8. Wang Tieying, Wang Yanwu, Wang Huanding. (2005). Research on hysteretic characteristics of two kinds of vertical lead dampers. *World Information on Earthquake Engineering* **21:1**, 134-139.
 9. Wang Yanwu, Wang Tieying, Wang Huanding. (2005). Experimental study of mechanical properties of steel-lead mixed dampers. *Engineering Mechanics* **22:2**, 149-154.
 10. Xin Yajun. (2005). Experimental study and theoretical analysis of new combined steel-lead damper. Harbin Institute of Technology, Harbin.
 11. Xin Yajun, Wang Huanding, Cheng Shuliang. (2007). Experimental study of new combined steel lead damper. *Engineering Mechanics* **24:3**, 126-130.
 12. GB 50011-2001. (2001). Code for seismic design of buildings.